Nanoscale

RSC Publishing

PAPER

View Article Online
View Journal | View Issue

Tracking the intracellular drug release from graphene oxide using surface-enhanced Raman spectroscopy†

Cite this: *Nanoscale*, 2013, **5**, 10591

Jie Huang,[a] Cheng Zong,[b] He Shen,[a] Yuhua Cao,[a] Bin Ren*[b] and Zhijun Zhang*[a]

We have developed a graphene oxide (GO)-based nanoplatform simultaneously loaded with a chemical drug and Ag nanoparticles (NPs), and employed it to study the drug release from GO in living cells by surface-enhanced Raman spectroscopy (SERS). In our strategy, doxorubicin (DOX), a typical model anticancer drug, was loaded onto chemically prepared GO by means of π–π stacking, while the Ag NPs were covalently modified onto GO. After incubation of the DOX- and Ag NPs-loaded GO with Ca Ski cells for several hours, DOX will detach from the GO in an acidic environment due to the pH-dependent π–π interaction between DOX and GO. Real-time measurement of SERS signals of DOX using the GO loaded with Ag NPs as a SERS-active substrate allows us to monitor the process of the drug release inside the living cell. The SERS results reveal that DOX is initially released from the GO surface inside the lysosomes, then escapes into the cytoplasm, and finally enters the nucleus, while GO, the nanocarrier, remains within the cytoplasm, without entering the nucleus.

Received 25th June 2013
Accepted 28th August 2013

DOI: 10.1039/c3nr03264g

www.rsc.org/nanoscale

1 Introduction

The development of nanoscale drug delivery systems has become a hot research field in nanomedicine because they can offer efficient and targeted drug transportation to specific disease sites, so as to reduce drug dosage and the severity of toxic side effects. Graphene oxide (GO) exhibits large surface area,[1] good biocompatibility and low toxicity after proper functionalization,[2,3] an ultrahigh drug loading ratio,[4] and has thereby become an ideal nanocarrier for drug delivery.[2–4] Doxorubicin (DOX) is a typical anti-cancer drug widely used in the treatment of many malignant diseases because of its broad antitumor activity.[5,6] Our previous work indicated that DOX can be efficiently loaded onto the GO surface by π–π stacking, with a loading ratio up to 400%.[4] The DOX molecules will detach from GO under acidic conditions because of the pH-dependent π–π stacking interaction between DOX and GO.[1,7] However, the precise process of drug release from GO inside the living cell has not been fully studied yet. Revealing this process is important to understand the mechanism of chemotherapy and for the design of novel, more efficient GO-based drug delivery systems.

The fluorescence technique has been used to monitor the drug delivery process.[8,9] However, fluorescent organic dye labeling has intrinsic limitations such as a broad fluorescence band, photo-bleaching, and interference from cellular auto-fluorescence. In TEM measurement, cells have to be sliced in the sampling process. Surface-enhanced Raman spectroscopy (SERS) has attracted considerable interest in life science due to it being non-destructive, showing resistance to photobleaching, narrow emission bands and ultrasensitive features.[10–12] SERS provides a "molecular fingerprint" that can be used to identify a molecule or verify its presence with its intrinsic signals in a sample, cell, or cellular compartment. SERS can enhance the Raman signals of target species adsorbed on Ag or Au metallic nanostructures by as much as 6–14 orders of magnitude, which even allows the detection of single molecules.[13–15] With these excellent advantages, SERS has previously been used to detect the diffusion, cellular uptake and dynamics of drugs in living cells,[16,17] which demonstrates that SERS is capable of obtaining dynamic information of drug molecules in living cells. In our previous work,[18] we prepared Au NPs–GO composites *via* chemical conjugation, and observed strong SERS peaks of GO at 1330 cm^{-1} and 1600 cm^{-1} in living cells. In addition, we showed that the introduction of Au NPs onto the GO surface led to a significantly enhanced Raman signal of GO in living cells, compared to that with isolated GO.[18]

In this work, we designed a GO-based nanoplatform onto which the drug molecules and Ag nanoparticles (NPs) were loaded by π–π stacking and covalent conjugation, respectively. Here, Ag NPs instead of Au NPs served as the SERS-active

[a]*Suzhou Key Laboratory of Nanobiomedicine, Division of Nanobiomedicine, Suzhou Institute of Nano-Tech and Nano-Bionics, Chinese Academy of Sciences, Suzhou 215123, China. E-mail: zjzhang2007@sinano.ac.cn; Fax: +86-512-62603079; Tel: +86-512-62872556*

[b]*State Key Laboratory of Physical Chemistry of Solid Surfaces, College of Chemistry and Chemical Engineering, Xiamen University, Xiamen 361005, China. E-mail: bren@xmu.edu.cn; Fax: +86-592-2181906; Tel: +86-592-2186532*

† Electronic supplementary information (ESI) available: Cytotoxicity of Ag–GO; SERS image after the cell incubated with Ag–GO for 2 h; fluorescence images of Ca Ski cells. See DOI: 10.1039/c3nr03264g

substrate, due to the much higher SERS enhancement of Ag NPs than Au NPs,[19] which will be better for detecting the Raman signals of DOX within cells. Here GO acts as a vehicle for loading and delivery of the Ag NPs and DOX into the cells. Through *in situ* detection of the SERS signals of DOX, and in combination with fluorescence microscopy, we investigated the release profile of DOX from GO inside living cells. Our results suggest that DOX was firstly detached from GO inside the lysosomes, escaped into the cytoplasm, and finally entered the nucleus; by contrast, GO was retained in the cytoplasm without entering the nucleus. Compared with the fluorescence technique, SERS allows a simple, rapid, non-destructive and direct analysis of the drug-release process inside living cells and tissues.

2 Experimental

2.1 Materials

Native graphite flakes were purchased from Alfa Aesar; *meso*-2,3-dimercaptosuccinic acid (DMSA), amine-terminated six-armed PEG, EDC, Lyso-Tracker® Green, Lyso-Tracker® Red and fluorescein isothiocyanate (FITC) were purchased from Sigma; $AgNO_3$, trisodium citrate, NaOH and other reagents were purchased from China National Medicine Corporation and used as received.

2.2 Preparation and DMSA modification of Ag NPs

20 nm Ag NPs were prepared according to the approach of Lee and Meisel.[20] Briefly, $AgNO_3$ aqueous solution (100 mL, 5.30×10^{-4} M) was heated to boiling with vigorous stirring, to which a trisodium citrate solution (5 mL, 1%) was then added. The mixture was kept boiling for 1 h. Next, the solution was allowed to cool to room temperature with continuous stirring.

As-prepared Ag NPs (20 mL) were then added to an aqueous solution of *meso*-2,3-dimercaptosuccinic acid (DMSA) (2 mL, 0.2%) at pH 8.0 adjusted with NaOH. The obtained NPs were then separated and purified by centrifugation at 13 000 rpm for 20 min and washed three times with ultrapure water to remove the unbound DMSA. The resulting DMSA-modified Ag NPs were suspended in ultrapure water (20 mL).

2.3 Preparation of PEG-modified GO

GO was prepared by vigorous oxidation of graphite according to a modified Hummer's method.[21,22] To impart biocompatibility and physiological stability, GO was conjugated with amine-terminated six-armed PEG molecules *via* EDC chemistry.[23] The obtained PEG-GO was purified by centrifugation and dialysis.

2.4 Synthesis of Ag–GO composites

Assembly of Ag NPs onto the GO surface was achieved by chemical coupling of PEG-GO and DMSA-modified Ag NPs in the presence of EDC (Fig. 1A). In our experiment, 2 mL aqueous solution of PEG-GO (1.0 mg mL^{-1}) and 40 mg EDC were added to 20 mL aqueous solution of Ag NPs. The mixed solution was stirred at room temperature for 48 h, and then centrifuged at 13 000 rpm for 20 min, and washed with ultrapure water three times to remove the unbound GO and EDC. The resulting Ag–GO was very stable in the cell medium. Formation of Ag–GO was characterized by TEM. TEM images (Fig. 1B) were obtained using a Tecnai G2 F20 S-Twin transmission electron microscope.

To load DOX onto GO, 1 mL of doxorubicin hydrochloride solution (2 mg L^{-1} dissolved in water) was added to 10 mL aqueous solution of Ag–GO which was first adjusted to pH 8.0 with triethylamine in order to guarantee that more DOX can adsorb on GO, before being stirred for 12 h in a dark room. The free DOX was then removed by ultrafiltration through a 100 kDa filter (Millipore) until the filtrate was nearly colorless. The remaining Ag–GO/DOX solution was resuspended in ultrapure water. The concentration of the final DOX adsorbed on Ag–GO was estimated by UV-vis spectroscopy. The concentration of DOX was determined to be 131.7 μg mL^{-1}, and the loading capacity of DOX on GO (the weight ratio of loaded drug to carriers) was estimated to be 61.2%.

For confocal fluorescence microscopy imaging, the Ag–GO composites were labeled using fluorescein isothiocyanate (FITC) following the standard procedure: FITC (5 mg) was added to ultrapure water (1 mL), the undissolved FITC was removed by filtering, and the supernatant was added to 2 mL aqueous solution of Ag–GO. The mixture was stirred for 12 h in a dark room. Free FITC was removed by ultrafiltration through a 100 kDa filter until the filtrate was nearly colorless. The remaining Ag–GO/FITC solution was resuspended in ultrapure water.

2.5 Test of time-dependent drug release in aqueous solution

Ag–GO/DOX was dissolved in PBS and was characterized by UV-vis spectroscopy. The solution was divided into four equal parts and every part was acidified using drops of acetic acid until the pH reached 5.0. After that it was stirred for several hours. The four mixtures underwent ultrafiltration through a 100 kDa filter and washed several times to remove the free DOX that detached from the GO at 1 h, 2 h, 4 h and 6 h, respectively. The release process was monitored by UV-vis spectroscopy.

2.6 Cell incubation with Ag–GO

The Ca Ski cell line (human cervical carcinoma cell) was cultured in Dulbecco's modified eagle's medium (DMEM) with 10% fetal bovine serum (FBS). The cells were seeded in tissue culture flasks (about 3×10^5 cells) and incubated in a fully humidified atmosphere at 37 °C containing 5% CO_2. For SERS measurement, the cells were incubated on a glass slide overnight at 37 °C, then the culture medium was removed, and then fresh medium and the Ag–GO composites were added to incubate for 2 h and 6 h, respectively. After being washed with PBS several times, the samples were ready for SERS measurement.

2.7 Raman imaging

All normal Raman and SERS imaging was performed using a fast laser Raman imaging microscope (Raman-11, Nanophoton Co.) with a 488 nm and 785 nm laser. The line-shaped laser spot was illuminated on the sample *via* a combination cylindrical

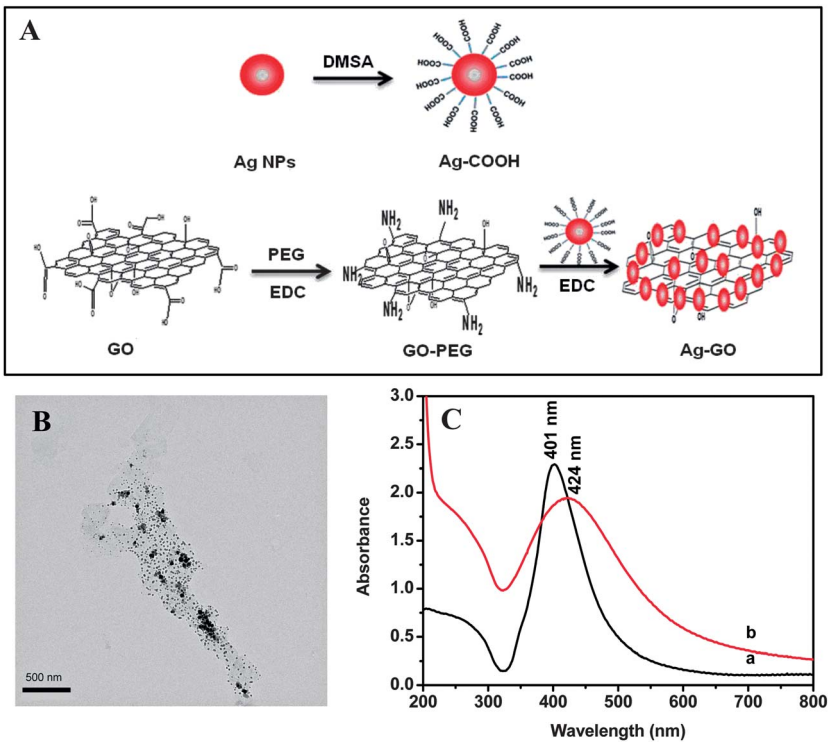

Fig. 1 (A) Schematic illustration of synthesis of Ag–GO composites. (B) TEM image of the composites of Ag NPs adsorbed on graphene oxide (Ag–GO). (C) UV-vis spectra of aqueous solution of (a) Ag NPs and (b) Ag–GO composites.

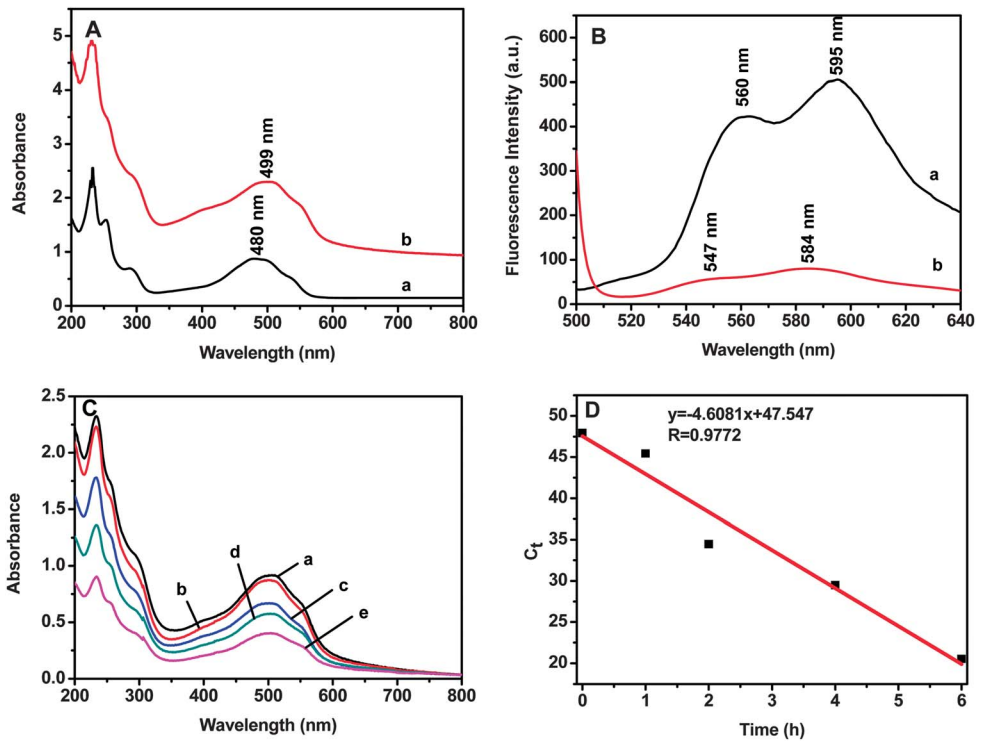

Fig. 2 UV-vis (A) and fluorescence (B) spectra of free DOX (a) and Ag–GO/DOX (b) in aqueous solution. Time-dependent drug-release at pH = 5.0. (C) UV-vis spectra of Ag–GO/DOX in acidic solution for (a) 0 h, (b) 1 h, (c) 2 h, (d) 4 h and (e) 6 h, respectively. (D) Plot of C_t *versus* time for the release process.

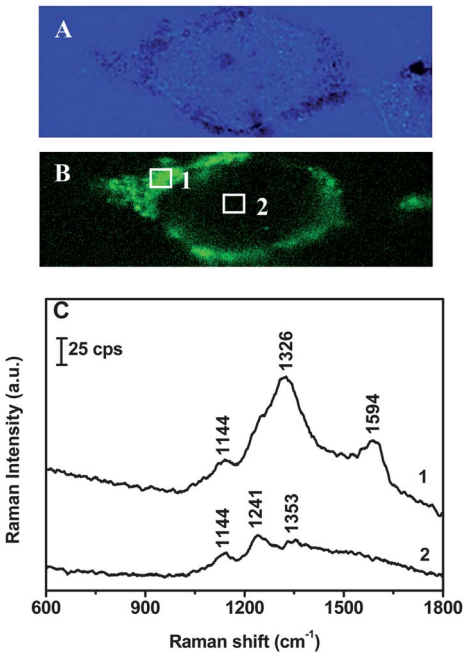

Fig. 3 (A) Bright field microscopic image of Ca Ski cells incubated with Ag–GO/DOX. (B) SERS image produced by the Raman band of GO at 1326 cm^{-1} (baseline corrected), excited with a 785 nm laser. (C) Mean SERS spectra obtained at the two different locations 1 and 2 in (B).

lens and line scanning optics. Raman scattering was detected by using an oil-immersion objective (100×, NA = 1.4). For Raman imaging, the line-focused laser was scanned by a galvanometer mirror at the sample plane. The grating is 300 gr mm^{-1}. The laser intensity at the sample plane is 0.1 mW μm^{-2} and the exposure time for each line is 1 s. The spectra were collected from 200 to 6000 cm^{-1}.

After being washed with PBS several times, the cover glass seeded with cells was put onto the sample stage (the side with cells up), then another cover glass was placed on top of it. The edges of the two cover glasses were further sealed using nail polish. After that, the sample was ready for normal Raman and SERS imaging.

2.8 Confocal fluorescence microscopy

Ca Ski cells were seeded in a 6-well plate at a density of 2×10^5 cells per well in 2 mL culture medium for 12 h. After that, the cells were incubated with Ag–GO/FITC for 3 h at 37 °C. The cells were then washed with DMEM. Finally, the DMEM was replaced with 2 mL Lyso-Tracker Red and incubated for a further 1 h at 37 °C. Then the cells were rinsed with PBS and observed under a laser confocal microscope (Nikon A1).

3 Results and discussion

3.1 Synthesis of Ag–GO

In this work, we prepared Ag–GO composites *via* chemical conjugation (Fig. 1A). TEM image shows that the GO sheets stack together, and that the Ag NPs (20 nm) formed aggregates on the GO surface (Fig. 1B). The aggregation of the metal NPs usually leads to strong SERS enhancement of the probe molecules.[18]

The binding of the Ag NPs to GO was also supported by UV-vis spectroscopy (Fig. 1C). The broadening and red-shift of the plasmon band of the Ag NPs in the Ag–GO composites, to that of the corresponding isolated Ag NPs, indicate the formation of the aggregated Ag NPs on the GO sheets, in agreement with the TEM result.

The biological toxicity of materials will influence the cell survival. WST assay indicates that the cytotoxicity of the Ag–GO (0.106 mM of Ag) was very low (Fig. S1 in the ESI†). Even though the Ca Ski cells were incubated with Ag–GO for 24 h, the relative cell viability rate still reaches 90%, indicating a very low cytotoxicity and good biocompatibility of Ag–GO.

3.2 Loading and release of anticancer drugs in an aqueous solution

GO has a long-range π conjugation that can interact with aromatic compounds *via* π–π stacking, which suggests potential applications as drug carriers.[1–3] In our experiment, the anticancer drug, DOX, was loaded onto GO *via* π–π interaction. The free DOX was removed from the solution by repeated centrifugation and filtration. UV-vis and fluorescence spectra of the resulting product were measured. The absorption peak at 499 nm and the emission peak at 584 nm suggest the formation of Ag–GO/DOX composites (Fig. 2A and 2B). A red-shift of the band due to DOX in the UV-vis spectra was observed after it was adsorbed on the Ag–GO composites (Fig. 2A). The quenching of the fluorescence of the DOX was observed after adsorption on Ag–GO (Fig. 2B), which is a result of the energy transfer between the DOX and Ag–GO (Förster resonance energy transfer).[24] In our previous work, the loading ratio of DOX on GO could reach 400%,[4] but in this experiment, the loading ratio of DOX on GO is only 61%, due to the occupation of the surface sites of GO by the Ag NPs.

DOX stacks onto GO *via* a π–π interaction. In PBS buffer, which is nearly neutral, DOX is stable on the GO surface; when the solution was adjusted to be more acidic, the amino group in the DOX molecules can be ionized, and then the aqueous solubility of DOX will increase, resulting in the detachment of DOX from the GO surface. To confirm this, we did an *in vitro* simulation experiment. Ag–GO/DOX was first dispersed in the acetic acid buffer (pH 5.0), then the solution was centrifuged and the free DOX was washed off. Centrifuging the solution at different times corresponded to different amounts of DOX detached from the Ag–GO. Then, the UV-vis spectra of the supernatant were recorded (Fig. 2C, spectra a–e). Our results clearly show that the release of DOX from GO speeds up in the acidic environment, with about 60% DOX released from the GO surface after 6 h in the acidic solution (Fig. 2D), whereas DOX would not release from Ag–GO in PBS buffer.[4]

3.3 Tracking the intracellular localization of Ag–GO by SERS

In our previous work, we confirmed that the amount of Au–GO uptake by Ca Ski cells reached the maximum at 6 h of incubation.[18] So we also incubated the Ca Ski cells with Ag–GO/DOX for

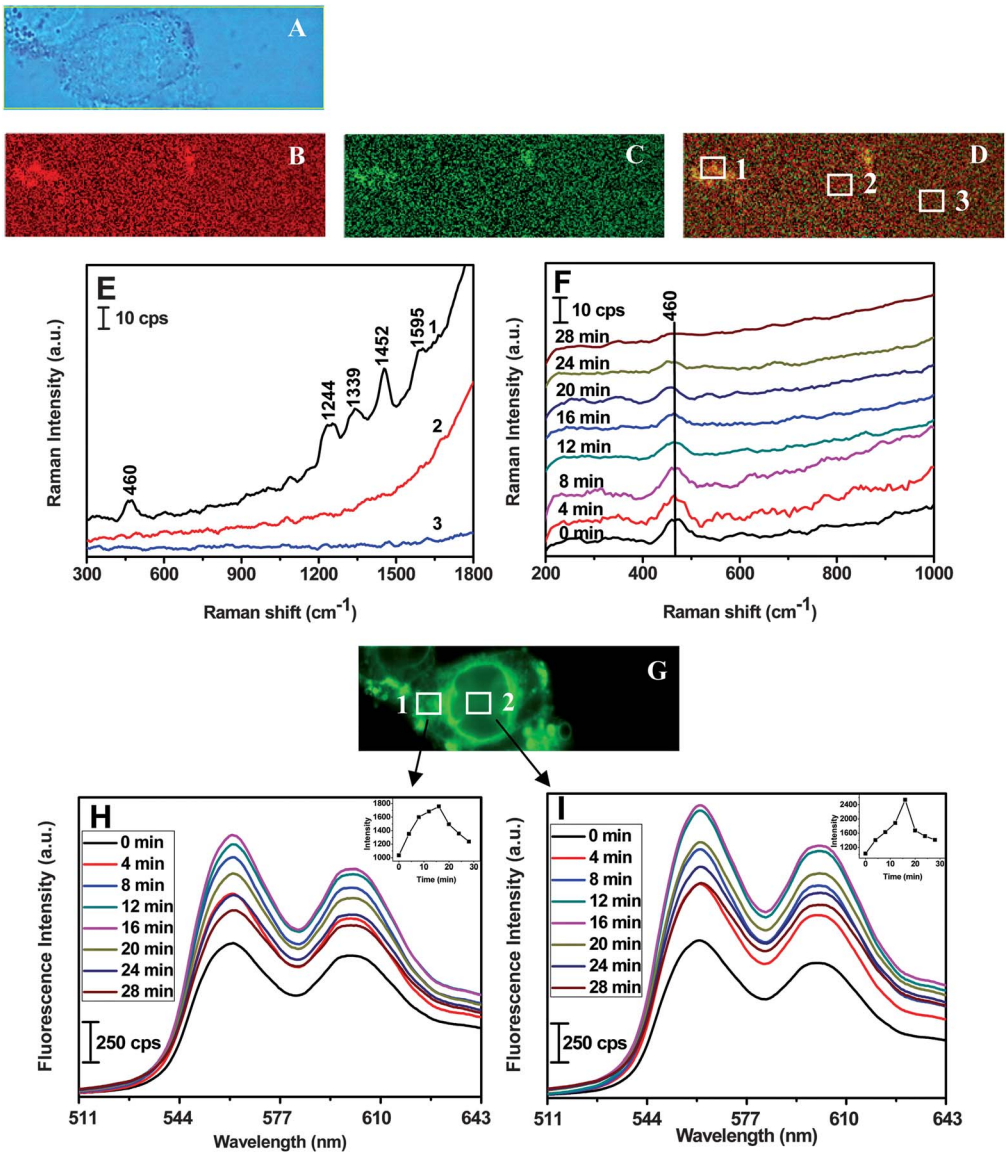

Fig. 4 (A) Bright field microscopic image of Ca Ski cells incubated with Ag–GO/DOX. (B) SERS image obtained simultaneously by the 460 cm^{-1} Raman band of DOX (baseline corrected). (C) SERS image produced simultaneously by the 1595 cm^{-1} Raman band of GO (baseline corrected). (D) Overlay of (B) and (C). (E) Mean SERS spectra obtained at three different locations (white frames 1, 2 and 3) of (D). (F) Mean SERS spectra obtained at white frame 1 of (D) at different times. (G) Fluorescence image constructed of the fluorescence band from 544 to 643 nm. (H) and (I) Mean fluorescence spectra obtained at white frames 1 and 2 of (G) at different times, respectively.

6 h. The bright field image in Fig. 3A shows one Ca Ski cell after 6 h of incubation with the Ag–GO/DOX. The SERS imaging was performed using the 1326 cm^{-1} band assigned to the D band of GO (Fig. 3B). The results show that some GO was internalized by the Ca Ski cell, and most of the GO was localized in the cytoplasm but not in the nucleus, which is consistent with the observation in our previous work.[18] Then we obtained the mean SERS spectra which consisted of 25 spectra lines of two different locations, respectively. One was from the cytoplasm (Fig. 3C, curve 1), and the other was from the nucleus (Fig. 3C, curve 2). The difference of the SERS spectra between the cytoplasm and nucleus is obvious. In the cytoplasm, we obtained the SERS spectra mostly from GO whereas we only obtained the Raman spectra of nucleotide and base in the nucleus. The peak at 1144 cm^{-1} corresponds to the ribose phosphate of nucleotides, and the peaks at 1241 cm^{-1} and 1353 cm^{-1} are assigned to the cytosine and adenine bases, respectively.[25] All these data suggest that GO did not enter the nucleus but only gathered in the cytoplasm.

3.4 Intracellular tracking of drug release from GO by SERS

To track the release process of DOX from the GO surface, Ca Ski cells were cultured with Ag–GO/DOX for 2 h, washed with PBS several times to remove physically adsorbed Ag–GO/DOX, and then the Raman spectra were recorded. The bright field image of the Ca Ski cell incubated with Ag–GO/DOX for 2 h is shown in Fig. 4A. We took the bands at 460 cm^{-1} and 1595 cm^{-1},

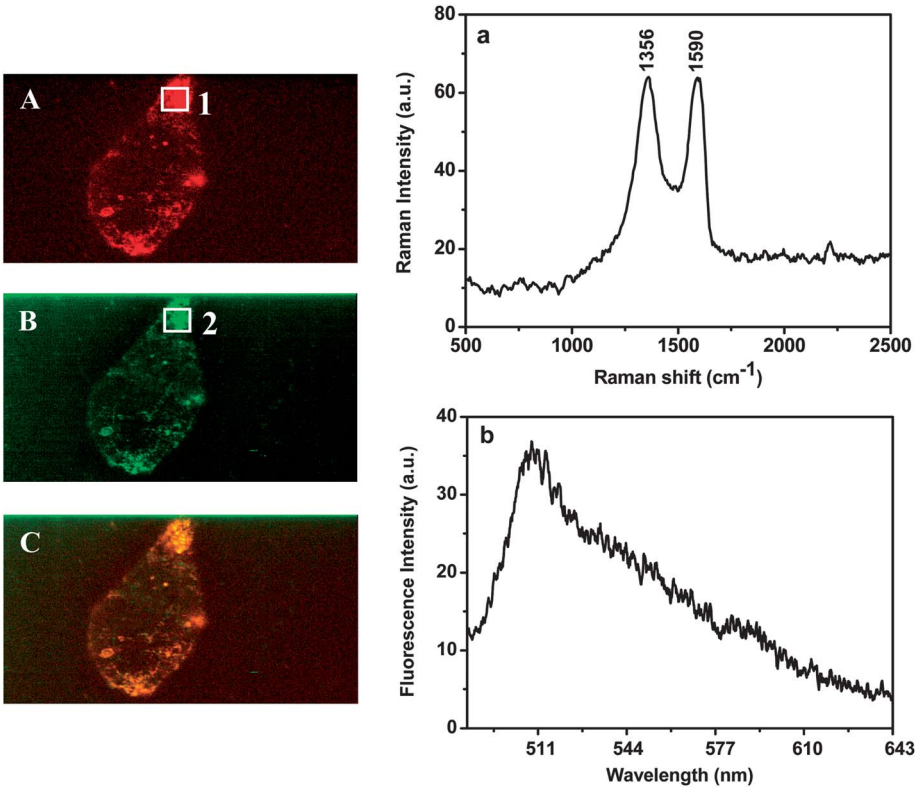

Fig. 5 (A) SERS image produced using intensity of the Raman band of GO at 1590 cm^{-1} (baseline corrected). (B) Fluorescence image produce by using 511 nm fluorescence band of Lyso-Tracker Green. (C) Overlay of (A) and (B). (a) and (b) are the corresponding mean spectra of (A; white frame 1) and (B; white frame 2), respectively.

characteristic of DOX and GO,[26] to construct the SERS images, respectively (Fig. 4B and 4C). Fig. 4D is the overlay of Fig. 4B and 4C, which indicates that the SERS spectra of DOX and GO match well. We recorded the mean SERS spectra of three different locations within one cell: one was from the cytoplasm (Fig. 4E, curve 1), the second location was from nucleus (Fig. 4E, curve 2), and the third spot was chosen from the substrate (Fig. 4E, curve 3), which correspond to the white frames 1, 2, and 3 in Fig. 4D, respectively. It can be seen from the two figures (Fig. 4D and 4E) that the Ag–GO/DOX composites were taken up by the Ca Ski cells after incubation for 2 h, and most of the DOX was still on the GO surface. Moreover, we can obtain the signals of the carrier by SERS easily without any dye labeling. We performed SERS mapping of DOX using the band of 460 cm^{-1} every 4 min. The mean SERS spectra of the DOX (white frame 1 in Fig. 4D) show that the SERS intensity decreased from 0 min to 24 min (Fig. 4F), and the SERS signal of DOX disappeared at 28 min (Fig. 4F and S2 in the ESI†). This means that the amount of DOX loaded on the GO surface decreased. We then studied the mean fluorescence spectra of DOX in the cytoplasm (white frame 1 in Fig. 4G) and nucleus (white frame 2 in Fig. 4G). It was found that the fluorescence intensity of DOX both in the cytoplasm (Fig. 4H) and the nucleus (Fig. 4I) first increased and then reached its strongest at 16 min, and after that the fluorescence was weakened. From this phenomenon we speculated that the DOX was released from the GO surface, and then entered

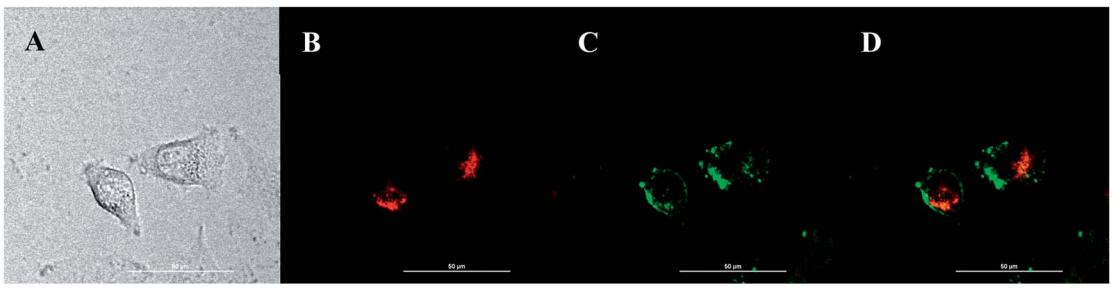

Fig. 6 Confocal fluorescence images of Ca Ski cells incubated with Ag–GO/FITC for 3 h, after which the lysosomes were stained with Lyso-Tracker Red. (A) Bright field microscopic image of Ca Ski cell, (B) Lyso-Tracker Red staining, (C) Ag–GO/FITC staining, and (D) overlay of (B) and (C). (Scale bar = 50 μm.)

cytoplasm and nucleus during the time from 0 to 16 min. Therefore, the originally quenched fluorescence signal was recovered after DOX was released from the GO surface, resulting in the increase in the fluorescence intensity of DOX in both the cytoplasm and the nucleus, and the decrease in the SERS intensity of DOX. After that, the DOX fluorescence may be photobleached by continuous laser excitation,[27] resulting in the decrease of the fluorescence intensity of DOX as well as the SERS intensity of DOX, and the latter finally disappeared. The fluorescence of DOX in the nucleus was stronger than that in the cytoplasm, confirming that most DOX entered nucleus finally. We examined the fluorescence intensity of the Ca Ski cell before and after incubation with Ag–GO using the same laser intensity, and the data demonstrated that the autofluorescence of the Ca Ski cell was weak under our experimental conditions, and this was also confirmed by the 3D image of living cells (Fig. S3 in the ESI†).

Previous studies have confirmed that DOX absorbed on carbon nanotubes can release in the intracellular lysosomes due to the acidic environment in the lysosomes after being delivered into the cells.[28] Our previous work indicates that GO is internalized by cells mainly through clathrin-mediated, energy-dependent endocytosis, which would go through the lysosomes.[18] In order to confirm whether or not the DOX loaded on GO will enter lysosomes and release from GO in lysosomes, we dyed the lysosome with Lyso-Tracker Green after incubation of the Ca Ski cells with Ag–GO for 2 h. Fig. 5A shows the SERS image obtained using the baseline corrected intensity of the GO band at 1590 cm^{-1}. Fig. 5B is the fluorescence image constructed by using the fluorescence band of Lyso-Tracker Green at 511 nm. Fig. 5C presents the overlay of Fig. 5A and 5B. The three images show that almost all of the Ag–GO entered into the lysosomes after 2 h of incubation, resulting in the DOX release from the GO surface. To confirm the SERS result, we employed confocal fluorescence microscopy to monitor the cellular uptake process of Ag–GO and to verify whether or not it enters into the lysosomes. In our experiment, Ag–GO was first labeled with fluorescein isothiocyanate (FITC) by covalent conjugation. Then the lysosomes were dyed with Lyso-Tracker Red after incubation of the Ca Ski cells with Ag–GO/FITC for 3 h. Merged confocal microscope images of the Ca Ski cell showed a strong green fluorescence as well as red fluorescence (Fig. 6), indicating the Ag–GO/FITC was internalized in the lysosomes, where efficient DOX release occurred. In addition, it was noted that binding of FITC to Ag–GO leads to a lower zeta potential (−23.2 mV) than that of Ag–GO (−15.7 mV), and thus it takes a longer time (3 h) for Ag–GO/FITC to enter the cells than does Ag–GO (2 h).

From the above results about the intracellular behavior of drug-loaded GO, we can propose a mechanism of drug release inside the cell. Firstly, the Ag–GO/DOX is taken up by cells through endocytosis and then captured into the lysosomes; after that, due to the acidic environment in the lysosomes, DOX starts to detach from the GO and escapes from the lysosomes to the cytoplasm to yield free DOX. The free DOX inside the cytoplasm finally enters the nucleus, while GO, the drug vector, mostly remains in the cytoplasm.

4 Conclusions

We designed and synthesized the Ag–GO composite *via* covalent conjugation, and employed it to study the release behavior of anticancer drug DOX from GO carriers in living cells by means of surface-enhanced Raman spectroscopy. Our results showed that after cellular uptake of DOX and Ag-loaded-GO, DOX was released from GO inside the lysosomes, and then the free DOX molecules entered into the nucleus, while the GO sheets were trapped in the cytoplasm. The current work may provide insight into the mechanisms of drug release from GO inside the living cells, which may guide the future design of more efficient GO-based drug delivery systems. Furthermore, we have demonstrated that SERS offers distinct advantages over the widely used fluorescence technique in that it can provide direct information on the carrier and the drug inside the living cells simultaneously, and with no need for dye labeling.

Acknowledgements

We acknowledge financial support of this work from NSFC (No. 21073224, 51361130033), MOST (2013CB933703), Innovation Project of CAS (KJCX2.YW.M12), and open project of State Key Laboratory of Physical Chemistry of Solid Surfaces at Xiamen University.

References

1 X. Y. Yang, X. Y. Zhang, Y. F. Liu, Y. F. Ma, Y. Huang and Y. S. Chen, *J. Phys. Chem. C*, 2008, **112**, 17554–17558.
2 Z. Liu, J. T. Robinson, X. M. Sun and H. J. Dai, *J. Am. Chem. Soc.*, 2008, **130**, 10876–10877.
3 X. M. Sun, Z. Liu, K. Welsher, J. T. Robinson, A. Goodwin, S. Zaric and H. J. Dai, *Nano Res.*, 2008, **1**, 203–212.
4 L. M. Zhang, J. G. Xia, Q. H. Zhao, L. W. Liu and Z. J. Zhang, *Small*, 2010, **6**, 537–544.
5 C. Tan, H. Tasaka, K. P. Yu, M. Murphy and D. A. Karnofsky, *Cancer*, 1967, **20**, 333–353.
6 J. R. Brown, *Prog. Med. Chem.*, 1978, **15**, 125–164.
7 D. Depan, J. Shah and R. D. K. Misra, *Mater. Sci. Eng., C*, 2011, **31**, 1305–1312.
8 M. Liong, J. Lu, M. Kovochich, T. Xia, S. G. Ruehm, A. E. Nel, F. Tamanoi and J. I. Zink, *ACS Nano*, 2008, **2**, 889–896.
9 J. M. Rosenholm, E. Peuhu, L. T. Bate-Eya, J. E. Eriksson, C. Sahlgren and M. Lindén, *Small*, 2010, **6**, 1234–1241.
10 J. J. Niu, M. G. Schrlau, G. Friedman and Y. Gogotsi, *Small*, 2011, **7**, 540–545.
11 R. M. Jarvis, N. Law, I. T. Shadi, P. O'Brien, J. R. Lioyd and R. Goodacre, *Anal. Chem.*, 2008, **80**, 6741–6746.
12 P. L. Stiles, J. A. Dieringer, N. C. Shah and R. P. Van Duyne, *Annu. Rev. Anal. Chem.*, 2008, **1**, 601–626.
13 S. M. Nie and S. R. Emory, *Science*, 1997, **275**, 1102–1106.
14 K. Kneipp, H. Kneipp, I. Itzkan, R. R. Dasari and M. S. Feld, *Chem. Rev.*, 1999, **99**, 2957–2975.
15 K. Kneipp, H. Kneipp, I. Itzkan, R. R. Dasari and M. S. Feld, *Chem. Phys.*, 1999, **247**, 155–162.

16 Š. Bálint, S. Rao, M. M. Sánchez, V. Huntošová, P. Miškovský and D. Petrov, *J. Biomed. Opt.*, 2010, **15**, 027005.
17 J. Yang, Y. P. Cui, S. F. Zong, R. H. Zhang, C. Y. Song and Z. Y. Wang, *Mol. Pharmaceutics*, 2012, **9**, 842–849.
18 J. Huang, C. Zong, H. Shen, M. Liu, B. Chen, B. Ren and Z. J. Zhang, *Small*, 2012, **8**, 2577–2584.
19 M. Fan, F. J. Lai, H. L. Chou, W. T. Lu, B. J. Hwang and A. G. Brolo, *Chem. Sci.*, 2013, **4**, 509–515.
20 P. C. Lee and D. Meisel, *J. Phys. Chem.*, 1982, **86**, 3391–3395.
21 W. S. Hummers and R. E. Offeman, *J. Am. Chem. Soc.*, 1958, **80**, 1339.
22 N. I. Kovtyukhova, P. J. Ollivier, B. R. Martin, T. E. Mallouk, S. A. Chizhik, E. V. Buzaneva and A. D. Gorchinskiy, *Chem. Mater.*, 1999, **11**, 771–778.
23 S. Stankovich, D. A. Dikin, G. H. B. Dommett, K. M. Kohlhaas, E. J. Zimney, E. A. Stach, R. D. Piner, S. T. Nguyen and R. S. Ruoff, *Nature*, 2006, **442**, 282–286.
24 Y. Wang, Z. H. Li, J. Wang, J. H. Li and Y. H. Lin, *Trends Biotechnol.*, 2011, **29**, 205–212.
25 R. R. Sathuluri, H. Yoshikawa, E. Shimizu, M. Saito and E. Tamiya, *PLoS One*, 2011, **6**, 22802–22814.
26 C. J. Lee, J. S. Kang, M. S. Kim, K. P. Lee and M. S. Lee, *Bull. Korean Chem. Soc.*, 2004, **25**, 1211–1216.
27 Q. Zhao, C. H. Huang and F. Y. Li, *Chem. Soc. Rev.*, 2011, **40**, 2508–2524.
28 B. Kang, J. Li, S. Q. Chang, M. Z. Dai, C. Ren, Y. D. Dai and D. Chen, *Small*, 2012, **8**, 777–782.